Surface Treatment and Doping Dependence of In_2O_3 Nanowires as Ammonia Sensors

Chao Li, Daihua Zhang, Bo Lei, Song Han, Xiaolei Liu, and Chongwu Zhou*

Department of E.E.-Electrophysics, University of Southern California, Los Angeles, California 90089

Received: July 23, 2003

Devices based on single-crystalline In_2O_3 nanowires were used to detect ammonia gas via electrical measurements at room temperature. Interesting phenomena have been observed, as the direction of the conductance modulation upon NH_3 exposure depends on both the initial state of the nanowire surface and the nanowire doping concentration. For nanowires with surfaces cleaned via UV illumination in a vacuum, the conductance has been found to increase for lightly doped nanowires and decrease for heavily doped nanowires upon exposure. In contrast, for nanowires residing in ambient atmosphere, i.e., under practical conditions, the conductance has been consistently observed to increase upon NH_3 exposure, regardless of the doping concentration. This is explained by considering electron transfer between In_2O_3 nanowires and NH_3. Our work clearly demonstrates the potential of using In_2O_3 nanowires as NH_3 sensors under practical conditions.

Nonstoichiometric metal oxide materials such as In_2O_3, ZnO, and SnO_2 films have been extensively studied to work as toxic chemical sensors,[1,2] among which ammonia gas sensors working under practical conditions are particularly interesting for industrial applications and environmental studies. Until now, most NH_3-sensing work is based on metal oxide films,[2] whose performance is severely hampered by the limited surface-to-volume ratios for thin films. An additional drawback for these thin-film sensors is that they have to operate at high temperatures (200−600 °C) to gain sufficient sensitivity, which brings significant inconvenience for practical applications.[2] These drawbacks can be overcome by using one-dimensional nanostructures such as nanowires or nanotubes boasting ultrahigh surface-to-volume ratios. Carbon nanotubes and SnO_2 nanobelts have been demonstrated to work as chemical sensors at room temperature.[3−5] More recently, we have demonstrated that In_2O_3 nanowire sensors show superior characteristics in many aspects for NH_3 detection, such as high on/off ratios and fast response.[6] An intriguing phenomenon of suppressed conduction upon NH_3 exposure was also observed for our n-type In_2O_3 nanowire devices pretreated with UV illumination,[6] in sharp contrast to the common belief that NH_3 should lead to enhanced conduction for In_2O_3 by working as a reducing agent and donate electrons. Furthermore, the interaction between NH_3 and In_2O_3 nanowires without UV pretreatment remains an open issue, as the moisture adsorbed on the nanowire surface may interfere with the NH_3 sensing process under practical conditions.

In this paper, we will present results from in-depth studies on In_2O_3 nanowire sensors working under practical conditions. We have studied both devices with clean surfaces, where UV pretreatment was employed to cleanse the adsorbed species such as oxygen and moisture (thus termed UV initialization), and devices exposed to ambient air without UV pretreatment (thus termed ambient air initialization). An intriguing interplay between the surface treatment and the nanowire doping concentration has been observed. For nanowires with surfaces cleaned via UV illumination in a vacuum, the conductance has been found to increase for lightly doped nanowires and to decrease for heavily doped nanowires upon exposure. In contrast, for nanowires residing in ambient atmosphere, i.e., under practical conditions, the conductance has been consistently observed to increase upon NH_3 exposure, regardless of the doping concentration. Furthermore, the interaction between our nanowires and oxygen has been found to be negligible compared to the interaction with ammonia. The significance and implication of our observation will be discussed.

Single-crystalline In_2O_3 nanowires were synthesized using a chemical vapor deposition system described previously,[7] where indium vapor was generated via laser ablation of an InAs target and oxygen mixed in argon was supplied for the production of In_2O_3. Our recent innovation involved using highly ordered pyrolytic graphite (HOPG) decorated with 10 nm gold clusters as our substrates, which produced nanowires with little byproducts, as shown in Figure 1a. As-grown In_2O_3 nanowires distributed uniformly across the HOPG substrate, and appeared homogeneous and straight with lengths up to several micrometers and diameters around 10 nm. Figure 1b shows a transmission electron microscope (TEM) image of a single In_2O_3 nanowire with a diameter of 10 nm, where the In/Au alloy particle can be seen at the tip of the wire. The nanowire diameter (∼10 nm) is apparently consistent with the diameter of the catalytic particle. Figure 1b, upper inset, shows a selected area electron diffraction (SAED) pattern, recorded perpendicular to a nanowire long axis. Analysis of the SAED pattern revealed a single-crystalline cubic lattice with a lattice constant of 1.03 nm for our nanowires. In addition, indexing the pattern demonstrates that the [110] direction is the nanowire growth direction. A high-resolution TEM (HRTEM) image is shown in Figure 1b, lower inset. The lattice spacing along the [110] growth direction (0.72 nm) is in good agreement with the lattice constant for In_2O_3 (1.01 nm).[8] Furthermore, it is apparent from the HRTEM image that there is no amorphous layer outside our nanowire, as compared to nanowires made of Si and InP,[9] which are often surrounded by an amorphous native oxide layer. This important discrepancy leads to significant results such as reliable electrical contacts and superior chemical sensing properties for our In_2O_3 nanowires. To produce nanowires of different doping concentrations, we have used two different oxygen concentrations in our synthesis: 0.02% O_2 in Ar for

* Corresponding author. E-mail: chongwuz@usc.edu.

10.1021/jp0361531 CCC: $25.00
Published on Web 10/23/2003

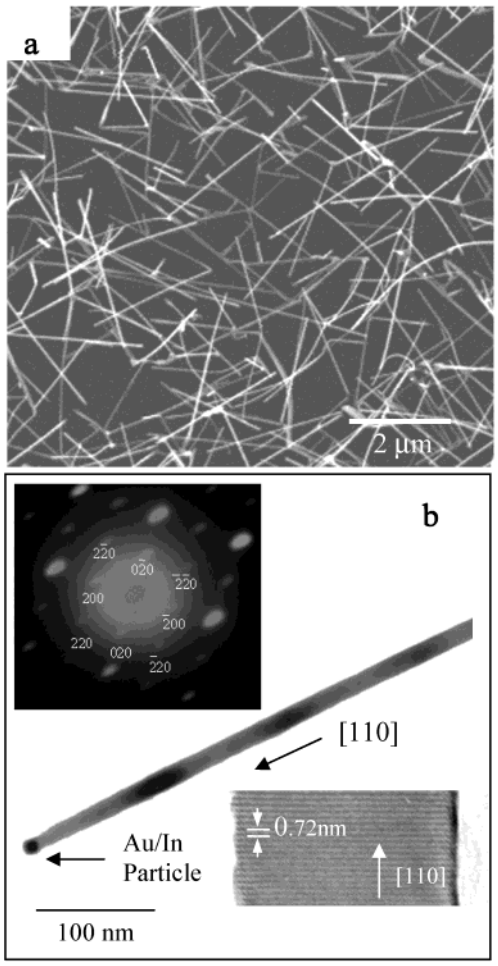

Figure 1. (a) SEM image of In_2O_3 nanowires grown on a HOPG substrate. (b) TEM image of an In_2O_3 nanowire with a catalyst particle at the tip. Upper inset: Electron diffraction pattern of the In_2O_3 nanowire. Lower inset: HRTEM image of an In_2O_3 nanowire showing the [110] growth direction.

high doping concentration and 0.04% O_2 in Ar for low doping concentration. The underlying mechanism is that doping in In_2O_3 is determined by the level of oxygen vacancies,[4−6] which is sensitive to the oxygen partial pressure during the synthesis. A similar technique has been used to produce In_2O_3 films of different electrical properties.[10] As-synthesized nanowires were deposited from a suspension in isopropyl alcohol onto a degenerately doped silicon wafer covered with SiO_2. Photolithography and Ti/Au deposition were performed to pattern the drain and source electrodes to contact both ends of individual wires. The Si substrate was used as a back gate in our electronic measurements. Figure 2a, inset, shows an SEM image of a typical In_2O_3 nanowire device, where a single nanowire bridging the source and drain electrodes can be clearly seen. These as-fabricated In_2O_3 nanowire devices exhibited typical n-type transistor characteristics, as a negatively increasing gate bias can reduce the conductance monotonically by several orders of magnitude.[11]

Our nanowire chemical sensing measurements were based on these In_2O_3 nanowire transistors by mounting them in a small chamber with electrical feed-through. Two methods have been used to initialize our devices before NH_3 exposure. One is called UV initialization, with which the system was usually pumped to vacuum, and then illuminated with UV ($\lambda = 254$ nm) to desorb oxygen and moisture species off the nanowire surfaces.[12] This cleansing effect of UV irradiation has been thoroughly studied before, including using spectroscopic techniques.[13] The devices were then exposed to NH_3 diluted in dry air, which was chosen to avoid the confounding effects of moisture. The second method is aimed at sensing applications under practical conditions and called ambient air initialization, meaning the sample was exposed to ambient air containing moisture. The devices were then exposed to both NH_3 diluted in dry air and NH_3 diluted in ambient air. A quantitatively similar sensing response was observed regardless of whether dry air or ambient air was used, presumably because the nanowire surface was already covered with moisture species before the exposure and hence appeared insensitive to the moisture in the ambient during the exposure. To simplify our discussion, only the results obtained with the devices exposed to NH_3 in dry air will be presented below, though we stress that our ambient air initialization mimics practical sensing conditions and the results obtained therein have great implication for practical applications. UV illumination has been used to recover our devices after each NH_3 exposure.[12] Altogether, eight nanowire devices (four synthesized using 0.02% O_2 in Ar and the rest using 0.04% O_2 in Ar) have been carefully studied. Consistent behavior was observed for nanowires of each category, and data from two representative devices (samples #1 and #2) are described below. The doping concentrations of these devices were determined by measuring the gated transport, as shown below. This technique has been extensively used to determine the doping concentration of many nanowire/nanotube systems.[11,14] Other techniques such as energy-dispersive X-ray spectroscopy (EDX) and photoluminescence do not have the precision required for this study.

Figure 2a shows current−voltage ($I-V$) curves recorded before and after exposing sample #1 with UV initialization to 1% NH_3 in dry air for 5 min with the gate bias $V_g = -1.5$ V. The $I-V$ curve recorded before the exposure is typical of our In_2O_3 nanowire field effect transistors (FETs). The asymmetry in the $I-V$ curve is due to the local gating effect, similar to the pinch-off effect of conventional silicon-based FETs. After the exposure, the device showed a 5-fold increase in conductance at $V = 1$ V, shown in Figure 2a. Furthermore, we have also measured $I-V_g$ curves using a fixed drain-source bias of 50 mV (shown in Figure 2b) under three circumstances, i.e., in a vacuum, after flowing dry air, and after exposure to 1% NH_3 in dry air. The device exhibited only a slight decrease in conductance after exposed to dry air, thus indicating a very limited effect for O_2 molecules. In sharp contrast, upon exposing the device to 1% NH_3 in dry air, a significant shift in the threshold voltage (V_T) from −1.5 V to −3.5 V was observed, in addition to a 5-fold increase in conductance. These results are quite different from what we observed before,[6] where a suppression in conductance and a shift of V_T in the positive direction were observed.

Under practical conditions, In_2O_3 nanowires are expected to have both oxygen and moisture adsorbed on the surface. While oxygen is confirmed to have a rather minor effect, moisture may adsorb as OH^- groups and interfere with the NH_3 sensing process. We have therefore tested sample #1 with ambient air initialization. Before NH_3 exposure, the device exhibited far less conduction with ambient air initialization (shown in Figure 2c) than with UV initialization (shown in Figure 2a), indicating that moisture, unlike oxygen, has an acute effect on In_2O_3 nanowires. This device was then exposed to 1% NH_3 in dry air. After the exposure, the device showed an enhancement of conductance around 2 orders of magnitude for $V = 0.3$ V, as shown in Figure 2c. In addition, a shift of the gate threshold voltage from − 0.3

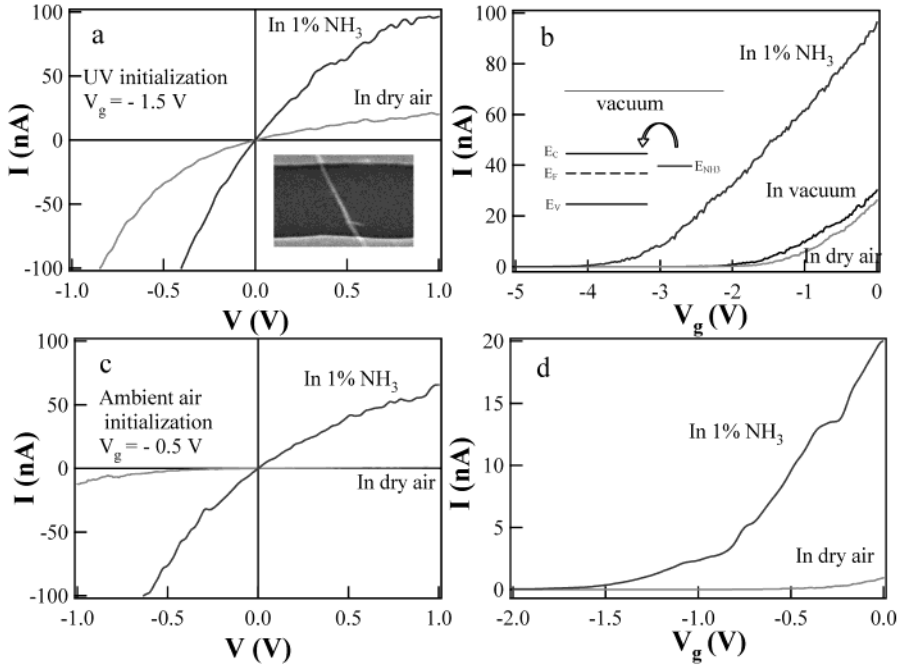

Figure 2. NH_3 sensing properties of sample #1. (a) $I-V$ curves taken before and after exposure to 1% NH_3 with UV initialization. Inset: SEM image of the device. (b) $I-V_g$ curves taken with the device residing in a vacuum, in dry air, and after the NH_3 exposure. Inset: band diagram of this device. (c) $I-V$ curves and (d) $I-V_g$ curves taken before and after the NH_3 exposure with ambient air initialization. In $I-V_g$ measurements, the drain−source bias was kept at 50 mV.

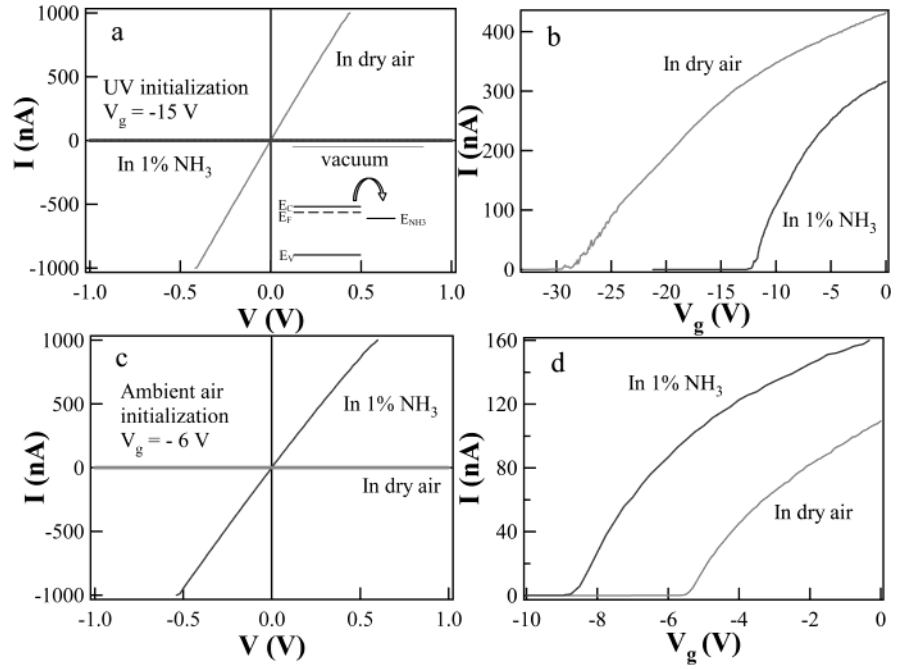

Figure 3. NH_3 sensing properties of sample 2. (a) $I-V$ curves and (b) $I-V_g$ curves taken before and after exposure to 1% NH_3 with UV initialization. Inset: band diagram of this device. (c) $I-V$ curves and (d) $I-V_g$ curves taken before and after exposure to 1% NH_3 with ambient air initialization. In $I-V_g$ measurements, the drain−source bias was kept at 50 mV.

V to −1.3 V was also observed upon NH_3 exposure, as shown in Figure 2d. Our results suggest that for sample #1, NH_3 donates electrons to the nanowire regardless of the surface preparation, thus leading to enhanced conduction under both UV and ambient air initialization. The change of carrier concentration after the exposure can be estimated to be $C\,\Delta V_T/eL \sim 5.04 \times 10^6$ cm^{-1} for UV initialization and 2.52×10^6 cm^{-1} for ambient air initialization, where ΔV_T is the shift of the threshold voltage, C is the capacitance of nanowire estimated to be 1.21×10^{-16} F, and L is the nanowire length ($\sim 3\ \mu m$).[14] Our results further suggest that, with moisture around, the electron transfer from ammonia to In_2O_3 nanowire is less efficient than without moisture (such as using UV initialization).

Similar measurements have been carried out with sample #2; however, a striking difference in response has been observed. Figure 3a shows the $I-V$ curves and Figure 3b shows the $I-V_g$ curves before and after exposure to 1% NH_3 in dry air with UV initialization. A significant suppression in conduction (up to 5 orders of magnitude at $V = 0.4$ V) has been observed after the exposure, accompanied by a pronounced shift of the threshold voltage (from −29 V to −11 V) toward the positive direction. This is qualitatively different from the results obtained

with sample #1, and is attributed to the difference in the nanowire doping concentrations, which can be estimated to be $n \equiv Q/eL = 2\pi\epsilon\epsilon_0 V_T/[e \ln(2h/r)] = 3.85 \times 10^6$ cm^{-1} (Figure 2b, $V_T = -1.5$ V, $r = 5$ nm, $h = 500$ nm) for sample #1 and 1.04×10^8 cm^{-1} (Figure 3b, $V_T = -29$ V, $r = 5$ nm, $h = 100$ nm) for sample #2, where ϵ_0 is the vacuum dielectric constant, ϵ is relative dielectric constant, L and r are the length and radius of the nanowire, respectively, and h is the thickness of the SiO_2 layer.[14] This discrepancy in doping was caused by different oxygen partial pressures used during the laser ablation process, as discussed before.

Two energy band diagrams are drawn in the inset of Figure 2b and Figure 3a for samples #1 and #2, respectively. E_c, E_v, and E_F correspond to the conduction band, the valence band, and the Fermi level of the In_2O_3 nanowires, and E_{NH_3} represents the chemical potential of the electrons in NH_3 that can participate in the electron-transfer process. Once NH_3 molecules adsorb onto the In_2O_3 nanowire surface, electrons transfer from the material with higher chemical potential to the material with lower chemical potential until the system reaches equilibrium. Our hypothesis is that for sample #2, the heavily doped device, the nanowire Fermi level E_F is fairly close to the conduction band and located above E_{NH_3} (Figure 3a, inset). Therefore electrons should migrate from the nanowire to the adsorbed NH_3 species and result in a reduction in the nanowire carrier concentration. This effectively leads to the observed suppressed conductance for sample #2. In contrast, a relatively low doping concentration was found for sample #1, suggesting E_F is way below the conduction band, presumably even below E_{NH_3}. As a result, electrons transfer from the adsorbed NH_3 molecules into the In_2O_3 nanowire and hence enhanced conduction was observed after the exposure. This hypothesis is backed by our calculation on the difference between E_c and E_F values for samples #1 and #2, which is estimated to be $(E_c - E_F)_{sample1} - (E_c - E_F)_{sample\ 2} = kT \ln(n_2/n_1) = 85.7$ meV, where n_1 and n_2 are the electron concentration for samples #1 and #2, respectively. This value is significant even at room temperature and may very well cause the electron transfer in opposite directions for nanowires with different doping concentrations. A thorough and quantitative understanding of this effect awaits theoretical calculations on the band alignment and electron-transfer ratios between In_2O_3 nanowires and NH_3.

Thus far, the doping-dependent sensing response for In_2O_3 nanowire transistors with UV initialization has been fully elucidated; however, for sample #2 with ambient air initialization, enhanced conduction and a negative shift of V_T (from -5.3 V to -8.7 V) have been observed after exposure to 1% NH_3 in dry air, as shown in Figure 3c,d. This seemingly odd behavior can actually be explained in a way similar to the doping-dependence. Even though the device carries a high doping concentration after UV initialization, a relatively low carrier concentration can be derived to be 1.9×10^7 cm^{-1} for the same device after the ambient air initialization. This low carrier concentration is a direct result of the moisture adsorbed on the nanowire surface when residing in ambient air and implies a band structure similar to the one depicted in Figure 2b, where E_F is below E_{NH_3} and hence electrons transfer from NH_3 to the nanowire upon exposure. Our results have significant implication for In_2O_3 nanowires working as chemical sensors under practical conditions; even though devices with UV initialization can exhibit either enhanced or suppressed conduction upon NH_3 exposure depending on the doping concentration, devices with ambient air initialization always exhibit enhanced conduction regardless of the original doping concentration.

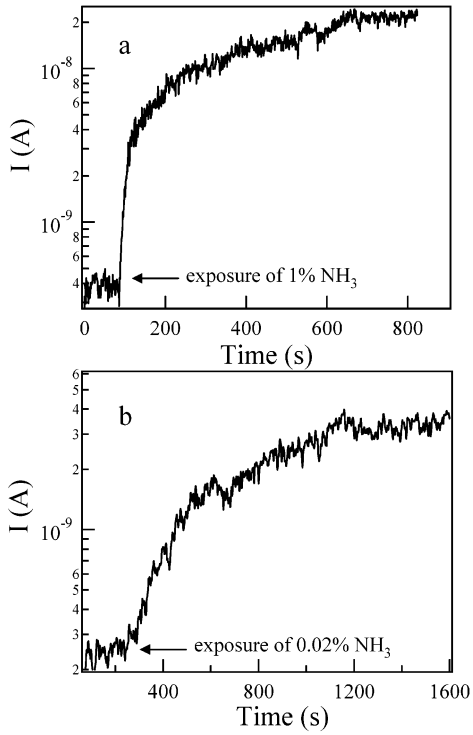

Figure 4. Time domain measurements of device exposed to 1% NH_3 (a) and 0.02% NH_3 (b). Here, $V_g = 0$ V, and $V = 0.3$ V.

The response time of our In_2O_3 nanowire transistors with ambient air initialization have also been studied. Figure 4a shows the response (current in log scale) of sample #1 to 1% NH_3 in dry air with $V_g = 0$ V and $V = 0.3$ V. A sharp increase in current was observed, and detailed analysis revealed a response time (defined as the time for the conductance to change by 1 order of magnitude) to 1% NH_3 less than 20 s and an on/off ratio approaching 50. The most diluted NH_3 we have tested was 0.02%, where the limitation was imposed by the availability of highly diluted NH_3 in air. Figure 4b shows a response time about 6 min for 0.02% NH_3.

In summary, we have found that the performance of In_2O_3 nanowires as NH_3 sensors is affected by both the doping concentration and the surface preparation. For devices with surfaces cleaned via UV illumination, devices with high doping concentrations exhibited reduced conductance and a shift of gate threshold voltage toward the positive side upon NH_3 exposure, while devices with lower doping concentrations displayed opposite behavior. However, with ambient air initialization, all devices showed enhanced conductance and a shift of the gate threshold voltage toward the negative side upon NH_3 exposure. It has also been found that oxygen has a relatively minor effect on the nanowire conductance, while moisture can reduce the nanowire conductance substantially. Furthermore, our nanowire sensors displayed on/off ratios $\sim$50 and response times $\sim$20 s with ambient air initialization for 1% NH_3. These results continue to demonstrate that In_2O_3 nanowires have significant potential as chemical sensors.

Acknowledgment. This work is supported by USC, a Powell award, NASA Contract NAS2-99092, an NSF CAREER award, NSF CENS program, and a Zumberge award.

References and Notes

(1) (a) Shimizu, Y.; Egashira, M. *MRS Bull.* **1999**, *24*, 18. (b) Williams, D. E. *Sens. Actuators, B* **1999**, *57*, 1. (c) Strassler, S.; Reis, A. *Sens. Actuators* **1983**, *4*, 465.

(2) (a) Liess, M. *Thin Solid Films* **2002**, *40*, 183. (b) Nanto, H.; Minami, T.; Takata, S. *J. Appl. Phys*. **1986**, *60*, 482.

(3) (a) Kong, J.; Franklin, N. R.; Zhou, C.; Chapline, M. G.; Peng, S.; Cho, K.; Dai, H. *Nature (London)* **2000**, *287*, 622. (b) Qi, P.; Vermesh, O.; Grecu, M.; Javey, A.; Wang, Q.; Dai, H.; Peng, S.; Cho, K. J. *Nano Lett*. **2003**, *3*, 347.

(4) Law, M.; Kind, H.; Messer, B.; Kim, F.; Yang, P. *Angew. Chem., Int. Ed.* **2002**, *41*, 2405.

(5) Comini, E.; Faglia, G.; Sberveglieri, G.; Pan, Z.; Wang, Z. *Appl. Phys. Lett.* **2002**, *81*, 1869.

(6) Li, C.; Zhang, D.; Liu, X.; Han, S.; Tang, T.; Han, J.; Zhou, C. *Appl. Phys. Lett.* **2003**, *82*, 1613.

(7) Li, C.; Zhang, D.; Han, S.; Liu, X.; Tang, T.; Han, J.; Zhou, C. *Adv. Mater*. **2003**, *15*, 143.

(8) Wyckoff, M. *Crystal Structures*; Interscience Publishers: New York, 1968.

(9) (a) Cui, Y.; Zhong, Z.; Wang, D.; Wang, W.; Lieber, C. M. *Nano Lett*. **2003**, *3*, 149. (b) Duan, X.; Huang, Y.; Cui, Y.; Wang, J.; Lieber, C. M. *Nature (London)* **2001**, *409*, 66.

(10) Gagaoudakis, G.; Bender, M.; Douloufakis, E., Katsarakis, N.; Natsakou, E.; Cimalla, V.; Kiriakidis, G. *Sens. Actuators, B* **2001**, *80*, 155.

(11) Zhang, D.; Li, C.; Han, S.; Liu, X.; Tang, T.; Jin, W.; Zhou, C. *Appl. Phys. Lett.* **2003**, *82*, 112.

(12) Zhang, D.; Li, C.; Han, S.; Liu, X.; Tang, T.; Jin, W.; Zhou, C. *Appl. Phys. A* **2003**, *77*, 163.

(13) (a) Rusu, C. N.; Yates, J. J. T. *Langmuir* **1997**, *13*, 4311. (b) Hoheisel, W.; Jungmann, K.; Vollmer, M.; Weidenauer, R.; Trager, F. *Phys. Rev. Lett.* **1988**, *60*, 1649.

(14) (a) Zhou, C.; Kong, J.; Yenilmez, E.; Dai, H. *Science* **2000**, *290*, 1552. (b) Martel, R.; Schmidt, T.; Shea, H. R.; Hertel, T.; Avouris, P. *Appl. Phys. Lett.* **1998**, *73*, 2447.